Chapter 1
THE DOUBLE SQUARE ROOT EQUATION AND RELATED OPERATORS

It is essential to the central topic of this thesis to develop the theory for the double square root equation. This equation describes downward continuation of both shots and receivers into the earth; thus it is of fundamental importance to seismic imaging. It is exact in the sense that it can handle all ranges of dip and offset angles. If we neglect the velocity gradient dv(z)/dz, the double square root equation is also exact for stratified earth and can be extended, with some caution, to treat lateral velocity variation, as will be shown in Chapter 3.

In this chapter, we will develop the basic 2-D theory for the double square root equation. This will allow a rigorous analysis of conventional seismic data processing. We will discover that conventional implementation of the double square root equation requires us to make zero-dip and zero-offset assumptions.

1-1 The Double Square Root Equation

We start with the scalar wave equation, which describes the propagation of the compressional wavefield P(x,z,t) in a medium with velocity v(x,z) and constant material density

$$\left[\frac{\partial^2}{\partial x^2} + \frac{\partial^2}{\partial z^2} - \frac{1}{v^2} \frac{\partial^2}{\partial t^2} \right] P = 0 \qquad (1\text{-}1)$$

Given the upcoming seismic wavefield $P(x,0,t)$ recorded at the surface, we would like to determine the reflectivity $P(x,z,0)$. This requires extrapolating the surface wavefield down to depth z and collecting it at $t = 0$.

It is to our advantage to decompose the wavefield into monochromatic plane waves with different angles of propagation from the vertical. Therefore, we would like to work in the Fourier domain whenever possible. We may Fourier transform the wavefield over time t. If we assume no lateral velocity variation, we may also Fourier transform over the horizontal axis x. Thus we have

$$P(k_x,z,\omega) = \iint P(x,z,t)e^{ik_x x - i\omega t}\, dx\, dt \qquad (1\text{-}2a)$$

and inversely,

$$P(x,z,t) = \iint P(k_x,z,\omega)\, e^{-(ik_x x - i\omega t)}\, dk_x\, d\omega \qquad (1\text{-}2b)$$

Applying the differential operator of (1-1) onto (1-2b), we get

$$\frac{\partial^2}{\partial z^2} P(k_x,z,\omega) + \left[\frac{\omega^2}{v^2} - k_x^2\right] P(k_x,z,\omega) = 0 \qquad (1\text{-}3)$$

For simplicity, let us further assume the constant velocity case. We will look into the case of stratified earth later in the section. The

upcoming wave solution to (1-3) can be immediately recognized as

$$P(k_x,z,\omega) = P(k_x,0,\omega)\, e^{-i\left[\frac{\omega^2}{v^2} - k_x^2\right]^{1/2} z} \qquad (1\text{-}4)$$

which is also the solution to the one-way wave equation

$$\frac{d}{dz} P(k_x,z,\omega) = -i\left[\frac{\omega^2}{v^2} - k_x^2\right]^{1/2} P(k_x,z,\omega) \qquad (1\text{-}5)$$

as may be readily verified by substituting (1-4) into (1-5). Let us define the vertical wavenumber as

$$k_z = -\frac{\omega}{v}\left[1 - \left(\frac{vk_x}{\omega}\right)^2\right]^{1/2} \qquad (1\text{-}6)$$

With this, Equation (1-4) takes the simple form

$$P(k_x,z,\omega) = P(k_x,0,\omega)\, e^{ik_z z} \qquad (1\text{-}7)$$

This equation has the physical implication that we seek : Given the wavefield recorded at the surface $P(x,0,t)$, we may double Fourier transform over (x,t) and get $P(k_x,0,\omega)$. Next, we simply multiply by the all-pass filter $\exp(ik_z z)$ to obtain the wavefield $P(k_x,z,\omega)$ at depth z. Subsequent inverse Fourier transformation over (k_x,ω) yields $P(x,z,t)$ from which we obtain the earth image $P(x,z,0)$. In practice, however, mapping is done in the transform domain directly from (k_x,ω) to (k_x,k_z) using (1-6) [Stolt, (1978)].

Our main objective here is to interpret (1-7) as a tool for downward extrapolating wavefields given at the surface. The first-year student of reflection seismology usually has difficulty in relating the simple mathematical development of the process presented above to its physics. Here is another, yet simpler derivation of Equation (1-7). We are given the upcoming wavefield recorded at the surface $P(x,0,t)$. Let us decompose this wavefield into monochromatic plane waves, each traveling at a different angle from the vertical. Hence, we identify these plane waves by attaching them to a unique (ω,k_x) pair of numbers. What we just did was Fourier transform the wavefield which is $P(k_x,0,\omega)$. Let us now consider one of these plane waves as depicted in Figure 1-1. Imagine that this plane wave passed a point P at $t = 0$, traveled upward, and was recorded by a receiver at the surface point A at time t. We would like to take the waveform at point A sitting on the wavefront at time t back to where it actually was; i.e. the reflection point P. It seems sensible to travel back using the same ray path. This means that downward continuation does not change the horizontal wavenumber k_x . Let us move the wavefront such that the waveform at A is now at A' at depth Δz . If we actually had a buried receiver at A' , it would have recorded our plane wave at $t - \Delta t$, where Δt is the traveltime between A - A' . In other words, going down Δz , we changed the traveltime by $-\Delta t$. From the geometry of Figure 1-1, we have

$$\Delta t = \frac{1}{v} \cos(\theta)\, \Delta z \qquad (1\text{-}8)$$

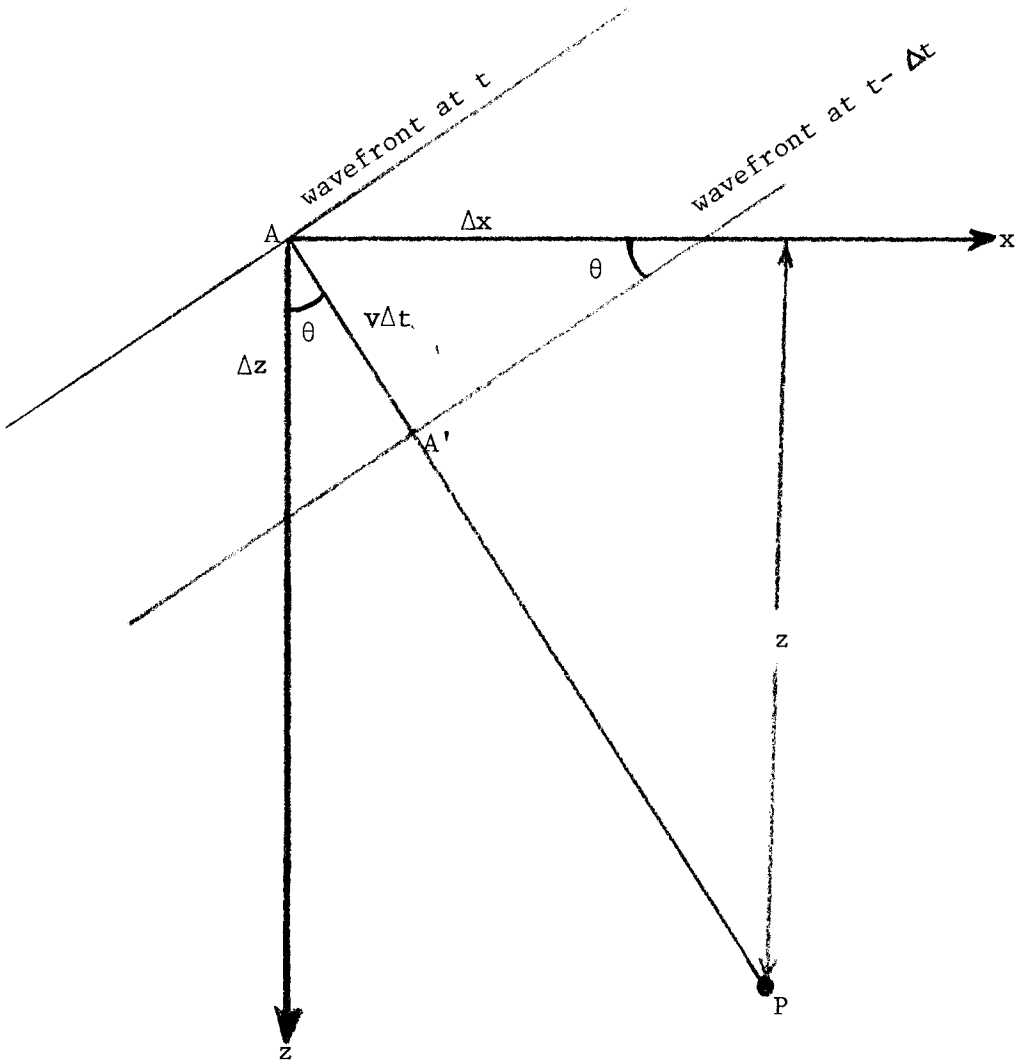

FIG. 1-1. On extrapolating wavefields.

where $v/\cos(\theta)$ is known as the vertical phase velocity. What we know about the plane wave is its k_x and ω. Suppose the distance between A - A' is λ wavelength. At time $(t - \Delta t)$, the wavefront intersects the x-axis at a distance of λ_x from A. Referring to the geometric relation in Figure 1-1

$$\frac{\lambda}{\lambda_x} = \sin(\theta) \tag{1-9a}$$

Thus, using the definitions $\lambda = 2\pi/(\omega/v)$ and $\lambda_x = 2\pi/k_x$, we obtain

$$\sin(\theta) = \frac{v\ k_x}{\omega} \tag{1-9b}$$

and

$$\cos(\theta) = \left[\ 1 - \left(\frac{vk_x}{\omega}\right)^2\ \right]^{1/2} \tag{1-9c}$$

where ω / v is the wavenumber along the ray path. Substituting (1-9c) into (1-8) we have

$$\Delta t = \frac{1}{v}\left[\ 1 - \left(\frac{vk_x}{\omega}\right)^2\ \right]^{1/2} \Delta z \tag{1-10a}$$

As we move down we do not want to change the wave amplitude. Given the change in traveltime $-\Delta t$ by (1-10a), the corresponding phase shift will simply be $-\omega\Delta t$. At each Δz -step of descent, we may assign a different velocity $v(z)$ to the waveform. This suggests that we change the angle (θ) from the vertical as we continue our journey along the ray path down to the destination point P. The total phase shift to which the waveform has been subject when we arrive at P is $-\int\omega dt$. In Fourier domain, all we have to do is multiply the transformed surface wavefield $P(k_x,0,\omega)$ by

$$e^{-i\int_A^P \omega\, dt} = e^{-i\int_0^z \frac{\omega}{v(z)}\left[1-\left(\frac{v(z)k_x}{\omega}\right)^2\right]^{1/2} dz} \qquad (1\text{-}10b)$$

which is exactly what Equation (1-7) implies, except that (1-7) was derived for constant v.

How do we know that we reached our destination point P and did not pass beyond it? Seismic imaging is not completed unless we impose a stopping condition onto downward continuation. Here, we simply terminate the process when our clock, which measures $t - \int \Delta t$, reads zero traveltime. Notice that the normalized wavenumber $X = vk_x/\omega$ is the sine of the angle of arrival to the receiver at A [Equation (1-9b)]. In fact, we will define extrapolation operators in the simple form involving only the cosine-like term $Op(X) = (1 - X^2)^{\frac{1}{2}}$, in which case $k_z = -(\omega/v)\, Op(X)$. This completes our discussion of the fundamentals of seismic imaging.

Let us utilize these concepts to downward continue a complete seismic experiment with many shots and receivers. We would like to downward continue both shots and receivers. First, consider a continuous stretch of receivers, each with a unique location g, along the x-axis. Then, we can use (1-7) together with (1-6), by replacing x with g, to downward continue these receivers. We use the reciprocity principle and

interchange shots and receivers. We then proceed similarly on a continuous stretch of shots, each with a unique location s, along the x-axis. In shot-receiver space (1-7) will read as

$$P(k_g, k_s, z, \omega) = P(k_g, k_s, 0, \omega)\, e^{ik_z z} \qquad (1\text{-}11)$$

When all shots and receivers are at depth $\int dz$, the wavefield has undergone a total phase shift of $-\omega \int (dt_g + dt_s)$. The vertical wavenumber then becomes

$$k_z = -\frac{\omega}{v}\left\{\left[1 - \left(\frac{vk_g}{\omega}\right)^2\right]^{1/2} + \left[1 - \left(\frac{vk_s}{\omega}\right)^2\right]^{1/2}\right\} \qquad (1\text{-}12)$$

For convenience, we define the normalized shot and receiver wavenumbers as

$$\begin{bmatrix} G \\ S \end{bmatrix} = \frac{v}{\omega}\begin{bmatrix} k_g \\ k_s \end{bmatrix} \qquad (1\text{-}13a,b)$$

causing (1-12) to take the simple form

$$k_z = - \frac{\omega}{v} DSR(G,S) \qquad (1\text{-}14)$$

where

$$DSR(G,S) = (1 - G^2)^{1/2} + (1 - S^2)^{1/2} \qquad (1\text{-}15)$$

Upon substituting (1-14) into (1-11) we have

$$P(k_g,k_s,z,\omega) = P(k_g,k_s,0,\omega)\ e^{-i \frac{\omega}{v} DSR(G,S)\ z} \qquad (1\text{-}16)$$

which is the solution to the ***double square root equation***

$$\frac{d}{dz} P(k_g,k_s,z,\omega) = - i\frac{\omega}{v} DSR(G,S)\ P(k_g,k_s,z,\omega) \qquad (1\text{-}17)$$

Equation (1-16) describes downward continuation of both shots and receivers into the earth. We will refer to (1-15) as the double square root operator (DSR). For simplicity, we leave out the scaling wavenumber ω / v from the definition of DSR.

Let us now turn our attention to the case of a stratified earth. Since we have not Fourier transformed P over z, the one-way wave equation (1-5) is also valid for v(z)

$$\frac{d}{dz} P(k_x,z,\omega) = -i \left[\frac{\omega^2}{v(z)^2} - k_x^2 \right]^{1/2} P(k_x,z,\omega) \qquad (1\text{-}18)$$

in which case (1-6) becomes

$$k_z(z) = - \frac{\omega}{v(z)} \left[1 - \left(\frac{v(z)k_x}{\omega} \right)^2 \right]^{1/2} \qquad (1\text{-}19)$$

(1-18) has the following solution

$$P(k_x,z,\omega) = P(k_x,0,\omega)\, e^{i\int_0^z k_z(z)\, dz} \qquad (1\text{-}20)$$

which immediately verifies (1-18) when substituted. However, in order for this to be a proper wave solution, we also would like it to satisfy the two-way scalar wave equation (1-3). From (1-18)

$$\frac{d^2}{dz^2} P = i \frac{dk_z(z)}{dv(z)} \frac{dv(z)}{dz} P + i\, k_z(z) \frac{dP}{dz}$$

where $P = P(k_x,z,\omega)$. Substituting (1-18) for dP/dz

$$\frac{d^2}{dz^2} P = i \frac{dk_z(z)}{dv(z)} \frac{dv(z)}{dz} P - k_z^2(z) P$$

If we ignore the velocity gradient dv(z)/dz, the final expression is

$$\frac{d^2}{dz^2} P + k_z^2(z) P = 0$$

Substituting (1-19) into this expression, we have

$$\frac{d^2}{dz^2} P + \left(\frac{\omega^2}{v(z)^2} - k_x^2 \right) P = 0 \qquad (1\text{-}21)$$

which is identical to the scalar wave equation (1-3). Consequently, the double square root equation can be extended to the case of the stratified earth model if we neglect the vertical gradient of material velocity. This is in reality a less severe assumption to make than restricting the analysis to stratified earth, i.e. ignoring any lateral variation in velocity. The double square root equation (1-17) now becomes

$$\frac{d}{dz} P = -i \frac{\omega}{v(z)} \mathrm{DSR}[G(z),S(z)] P \qquad (1\text{-}22)$$

where

$$\begin{bmatrix} G(z) \\ S(z) \end{bmatrix} = \frac{v(z)}{\omega} \begin{bmatrix} k_g \\ k_s \end{bmatrix} \qquad (1\text{-}23a,b)$$

An attempt will be made in Chapter 3 to further extend the theory to the case of lateral variation in velocity.

The double square root operator (DSR) given by (1-15) is separable in terms of shot and receiver wavenumbers. This means that one can first organize the wavefield recorded at the surface into common receiver gathers and use the first part of the DSR operator to downward continue the receivers to depth z. Following this, one can reorganize the already downward-continued wavefield into common shot gathers and use the second part of DSR to downward continue the shots to depth z. Alternating between common receiver and common shot gathers, the entire seismic wavefield can be downward continued until imaging is accomplished. Although no approximation, apart from the stratified earth assumption, is made in this process, it is clear that, computationally, this approach can be exhausting. In fact, today's seismic data processing is essentially done in the space of midpoint y and (half-)offset h rather than in shot-receiver (s,g)-space. We therefore would like to put DSR defined by (1-15) into (y,h)-coordinates. This requires the following coordinate transformation:

$$\begin{bmatrix} y \\ h \end{bmatrix} = \frac{1}{2} \begin{bmatrix} g + s \\ g - s \end{bmatrix} \qquad (1\text{-}24)$$

The principal of invariance states that wavefields do not change under a coordinate transformation; thus

$$P(s,g,z,t) = P'(y,h,z,t) \qquad (1\text{-}25)$$

where z and t are invariant under the coordinate transformation.

Applying the chain rule to (1-25),

$$\frac{\partial P}{\partial s} = \frac{\partial P'}{\partial y}\frac{\partial y}{\partial s} + \frac{\partial P'}{\partial h}\frac{\partial h}{\partial s} \qquad (1\text{-}26a)$$

and

$$\frac{\partial P}{\partial g} = \frac{\partial P'}{\partial y}\frac{\partial y}{\partial g} + \frac{\partial P'}{\partial h}\frac{\partial h}{\partial g} \qquad (1\text{-}26b)$$

Using (1-24), we simplify these differentials and get

$$\frac{\partial P}{\partial s} = \frac{1}{2}\left[\frac{\partial P'}{\partial y} - \frac{\partial P'}{\partial h}\right] \qquad (1\text{-}27a)$$

and

$$\frac{\partial P}{\partial g} = \frac{1}{2}\left[\frac{\partial P'}{\partial y} + \frac{\partial P'}{\partial h}\right] \qquad (1\text{-}27b)$$

Fourier transforming both sides of (1-27) and canceling $P = P'$, we obtain the midpoint-offset wavenumbers in terms of shot-receiver wavenumbers:

$$\begin{bmatrix} k_g \\ k_s \end{bmatrix} = \frac{1}{2}\begin{bmatrix} k_y + k_h \\ k_y - k_h \end{bmatrix} \qquad (1\text{-}28a,b)$$

Multiplying by v / ω , we normalize both sides and substitute (1-13) to get

$$\begin{bmatrix} G \\ S \end{bmatrix} = \begin{bmatrix} Y + H \\ Y - H \end{bmatrix} \qquad (1\text{-}29a,b)$$

where

$$\begin{bmatrix} Y \\ H \end{bmatrix} = \frac{v}{2\omega} \begin{bmatrix} k_y \\ k_h \end{bmatrix} \qquad (1\text{-}30a,b)$$

Final substitution of (1-29) into (1-15) yields the double square root operator in midpoint-offset space:

$$DSR(Y,H) = \left[1 - \left(Y + H \right)^2 \right]^{1/2} + \left[1 - \left(Y - H \right)^2 \right]^{1/2} \qquad (1\text{-}31)$$

The vertical wavenumber is now re-expressed in terms of normalized midpoint-offset wavenumbers Y and H

$$k_z = - \frac{\omega}{v} DSR(Y,H) \qquad (1\text{-}32)$$

Is (1-31) an improvement over (1-15)? We have lost the property of

separation in terms of spatial frequencies. Notice the strong coupling between Y and H. For instance, Taylor expansions of the square roots in (1-31) will yield terms containing cross products of the two wavenumbers. This in turn will require the recorded wavefield, which is now transformed into (y,h,t)-space, to be handled in its entirety, a problem we would like to avoid. In the next section, we will discover that conventional processing has a robust approach to this problem.

1-2 Conventional Processing

So far, we have developed an exact theory, namely the double square root equation, for the problem of seismic wavefield extrapolation. It will be beneficial to look into the conventional treatment of this problem, in order to determine whether these two approaches are completely alien to one another, or if they are related in some manner.

The conventional processing sequence comprises two major and crucial components. First, the data is organized into common midpoint (CMP) gathers and NMO correction is applied on each gather. The equation used for moveout correction is

$$\Delta t = t - t' = t' \left\{ \left[1 + \left(\frac{2\ h}{v\ t'} \right)^2 \right]^{1/2} - 1 \right\} \qquad (1\text{-}33)$$

where t is the two-way traveltime for a given (half-)offset h, and t' is the corresponding two-way zero-offset time. Total moveout correction is the difference between t and t' . In this equation, v is taken to be the RMS velocity at t' . Equation (1-33) is based upon the stratified earth (zero dip) assumption. The process implied by (1-33) simulates mapping of the CMP gather onto zero offset. Following the NMO correction, traces

of the CMP gather are stacked. This not only reduces the volume of the data but also enhances the signal-to-noise ratio.

The CMP stack is regarded as an upcoming wavefield recorded zero offset. This allows us to obtain the migrated section by downward extrapolation. The imaging condition is based on the so-called explosive reflectors model in that, at $t = 0$, the reflectors explode in unison sending an upcoming wave to the surface. Apart from being recorded on a one-way time scale, this wavefield is assumed to simulate a wavefield that would be recorded at zero offset. The equation used for downward extrapolation is the one-way wave equation (1-5). In order to account for the one-way traveltime of the explosive reflectors model, however, the velocity used in extrapolation is taken as half the medium velocity. Thus the vertical wavenumber given by (1-6) is re-expressed as

$$k_z = - \frac{2\omega}{v} \left[1 - \left(\frac{v\, k_y}{2\omega} \right)^2 \right]^{1/2} \qquad (1\text{-}34)$$

Since migration is done in midpoint space, we replaced k_x with k_y. Some of the current techniques of migration based on wave extrapolation utilize certain rational approximations to (1-34), and some implement the exact form in the frequency domain.

By now it is clear that conventional processing has an advantage over the exact theory represented by the double square root equation in midpoint-offset space. Unlike the latter, the conventional approach is composed of two separable operators, namely the NMO+stack applied in offset space and migration applied in midpoint space. However, we should be reminded that such an advantage is based on zero-dip and zero-offset assumptions. Where do we go from here? On the one hand, we have an exact theory that can handle all dips and offset angles, but is difficult to implement. On the other hand, we have a conventional approach

that has the convenient property of separation, but is based on assumptions which can be severe, particularly in a region with a complex structural setting. Should we drop both approaches and seek for another theory? No, let us find out whether these two approaches are related in any way. We will go back to the exact theory and make the same two assumptions which underlie the conventional approach.

The zero-dip assumption implies that the earth model is stratified. The seismic energy recorded over such an earth would be completely concentrated at the zero spatial frequency, in this case $k_y = 0$. This in turn suggests that we set the normalized wavenumber Y equal to 0 in DSR defined by (1-31). The resulting operator will be defined as the ***Stacking*** (St) operator, where

$$St(H) = 2 \left(1 - H^2 \right)^{1/2} - 2 \qquad (1\text{-}35)$$

The factor -2 may at first appear to be a post facto addition to St(H). But, let us think what we want to do with this operator. The first part of St(H) takes each shot-receiver pair on a CMP gather down to a reflecting point following raypaths with $\cos(\theta) = (1 - H^2)^{\frac{1}{2}}$. Next, we would like to come back up to the surface following a vertical path to the point halfway between the shot and receiver. This is simply equivalent to a constant phase shift (time retardation), which accounts for the factor -2.

As shown in Appendix B (Section B-2), it turns out that the NMO shift given by (1-33) is a stationary phase approximation to (1-35). What the operator St(H) does is condense primary information on a CMP gather down to zero offset. As far as this operator is concerned, stacking amounts to selecting off the zero offset and abandoning all other offsets. Therefore, (1-35) is a zero-dip NMO+stack-type operator.

Incorporating the zero-offset (h = 0) assumption into the double

square root operator is relatively more subtle. On a CMP gather, at and near h = 0, energy is essentially concentrated at zero spatial frequency, in this case $k_h = 0$. In fact, the task that the NMO correction attempts to accomplish is to push the primary energy on a CMP gather towards $k_h = 0$. So, setting the normalized offset wavenumber H = 0 in (1-31) we define the ***Explosive Reflectors*** (ER) migration operator as

$$ER(Y) = 2 \left(1 - Y^2 \right)^{1/2} \qquad (1\text{-}36)$$

Setting H = 0 in (1-32) we have the zero-offset vertical wavenumber

$$k_z = - \frac{\omega}{v} 2 \left(1 - Y^2 \right)^{1/2} \qquad (1\text{-}37)$$

Substituting the definition for $Y = v k_y / 2 \omega$ into (1-37) we obtain

$$k_z = - \frac{2 \omega}{v} \left[1 - \left(\frac{v k_y}{2 \omega} \right)^2 \right]^{1/2} \qquad (1\text{-}38)$$

which is identical to (1-34). Thus, we conclude that the zero-offset operator ER(Y) derived from the double square root equation is identical to the migration operator that is based on the explosive reflectors model of conventional processing.

Let us now define the following operator:

$$Sep(Y,H) = DSR(Y,H_o) + DSR(Y_o,H) - DSR(Y_o,H_o) \qquad (1\text{-}39)$$

where H_o and Y_o are scalars. In order to grasp the nature of the operator Sep(Y,H), let us consider the simplest case: if $H_o = Y_o = 0$, using the definition for DSR given by (1-31), we have

$$Sep(Y,H) = 2(1 - Y^2)^{1/2} + 2(1 - H^2)^{1/2} - 2 \qquad (1\text{-}40)$$

Adding (1-35) and (1-36) and comparing with (1-40) we have

$$Sep(Y,H) = ER(Y) + St(H) \qquad (1\text{-}41)$$

Hence, the operator Sep(Y,H) defined by (1-41) describes the total downward continuation involved in conventional processing. Certainly, when an imaging condition is imposed on this operator, the scaling wavenumber ω/v is different for the two components, namely St(H) and ER(Y). Notice that if Y = 0 we have , from (1-40) and (1-31),

$$Sep(Y=0,H) = DSR(Y=0,H) \qquad (1\text{-}42a)$$

and if H = 0 we have

$$Sep(Y,H=0) = DSR(Y,H=0) \qquad (1\text{-}42b)$$

However, if Y and H are both non-zero, the Sep(Y,H) operator fails to include terms with cross products of Y and H, which would be present in the Taylor series expansion of DSR(Y,H). It is the absence of such terms that makes it possible to express Sep(Y,H) in the separable form (1-40). The generalized expression (1-39) for Sep(Y,H) allows us to define other forms of separable approximations to DSR by assigning non-zero values to H_o and/or to Y_o.

In conclusion, we made a rigorous analysis of conventional processing and showed that it can be developed from the theory of the double square root equation. We discovered that conventional processing simply utilizes a separable approximation to DSR. The zero-dip and zero-offset assumptions are the basis for the separability. How severe are these assumptions? To answer this question, we are motivated to study the response characteristics of the DSR and Sep operators.

1-3 Response Characteristics of DSR(Y,H) and Sep(Y,H)

Transfer functions and impulse responses of the DSR and Sep operators are displayed in five different planes, namely

(1) k_y vs. ω for constant(z,h)

(2) k_y vs. z for constant (ω,h)

(3) y vs. z for constant (ω,h)

(4) y vs. z for constant(t,h)

(5) y vs. t for constant(z,h)

Many interesting observations can be made on these planes concerning characteristics of the operators of interest. We consider the following transfer functions

$$e^{i\frac{\omega}{v}\,DSR(k_y,k_h,\omega)z} \qquad (1\text{-}43a)$$

where

$$DSR(k_y,k_h,\omega) = \left[1 - \left(\frac{v\ k_y}{2\ \omega} + \frac{v\ k_h}{2\ \omega} \right)^2 \right]^{1/2} + \left[1 - \left(\frac{v\ k_y}{2\ \omega} - \frac{v\ k_h}{2\ \omega} \right)^2 \right]^{1/2} \qquad (1\text{-}43b)$$

and

$$e^{i\frac{\omega}{v} Sep(k_y,k_h,\omega)z} \qquad (1\text{-}44a)$$

where

$$Sep(k_y,k_h,\omega) = 2 \left[1 - \left(\frac{v\ k_y}{2\ \omega} \right)^2 \right]^{1/2} + 2 \left[1 - \left(\frac{v\ k_h}{2\ \omega} \right)^2 \right]^{1/2} \qquad (1\text{-}44b)$$

Here we used the definitions for Y and H from (1-30). Inverse Fourier transforming (1-43a) and (1-44a) over k_y,k_h and ω yields the impulse response of each of the extrapolation filters (1-43a) and (1-44a). Notice that (1-44b) is the non-retarded Sep operator.

In the following figures, discretization intervals were taken to be $\Delta y = \Delta h = \Delta z = 25$ m and $\Delta t = 16$ msec . The velocity of the medium is 3000 m/sec and the non-zero offset considered is h = 400 m. No attempt was made to remove wraparound effects in y, h and t.

Figure 1-2 shows the (ω,k_y) -plane for constant z and h. The transition boundary from the propagation to the evanescent region widens as

temporal frequency increases.

Figure 1-3 shows the (k_y,z) -plane for constant ω and h. Again the abrupt change at $k_y = 2\,\omega / v$ occurs due to transition from the propagation to the evanescent region. The zero-offset case (a) clearly shows evanescent energy dying off rapidly with depth. Moreover, the width of the propagation region stays constant with depth. The non-zero offset case (b), however, indicates that the width of the propagation region varies with depth, being zero at the surface and increasing rapidly and asymptotically to the zero-offset case. The physical interpretation of this depth-dependency is quite intuitive: H becomes less and less significant at greater depths and Y becomes the dominating wavenumber. On a CMP gather, moveout will decrease at great depths, implying a nearly zero spatial frequency k_h . Referring to the Sep operator (c), we do not observe such a variation in depth.

Figure 1-4 shows the (y,z) -plane for constant ω and h. The zero-offset case (a) represents the response of a monochromatic wave impinging on a point aperture. Note the circular wavefronts centered at the aperture. The amplitude on a particular wavefront is strongest on the z-axis, and dies off away from it. The non-zero offset case (b) shows elliptical wavefronts that are difficult to relate to a physical situation. The Sep operator (c) is trying and failing to simulate the elliptical wavefronts.

Figure 1-5 shows snapshot pictures of the (y,z)-plane at constant t and h. The zero-offset case (a) shows a circular wavefront, whereas the non-zero offset case (b) shows two elliptical wavefronts, one for h = 400 m and the other for h = 1200 m. The presence of the latter is due to wraparound in h. The (y,z)-plane for the Sep operator (c) also has two wavefronts, for h = 400 m and h = 1200 m. Although the wavefront for h = 400 m appears to be in good agreement with the true elliptical wavefront of (b) up to fairly wide angles from the vertical, the wavefronts associated with the far offset (h = 1200 m) are hardly in agreement at all.

Figure 1-6 shows the (y,t)-plane for constant h and z. Each figure is actually a superposition of four (y,t)-planes at different z-levels. These figures represent the impulse responses of DSR and Sep to point

scatterers buried at indicated depths z. The zero-offset case (a) has hyperbolic trajectories, while the non-zero offset case (b) has the well-known table top trajectories. The difference between the zero offset and the non-zero offset is quite evident, particularly for the two shallow scatterers. The moveout is also obvious as one compares the arrival times. In Appendix B (Section B-1), the circular and elliptical wavefronts of Figure 1-5 and the hyperbolic and table-top loci of arrivals in Figure 1-6 are confirmed by the stationary phase approximation to DSR. Although the Sep operator handles the NMO to a certain extent (perfect at the top of each trajectory) , it cannot account for the table-top trajectories indicated by the nonzero offset section (b). A stationary phase approximation to the Sep operator is also given in Appendix B (Section B-3).

In summary, response characteristics clearly demonstrate that the Sep operator does not handle wide offsets properly, especially in the shallow portion of common offset sections. In Chapter 2, we will develop a theory which will remedy this problem to a certain degree of accuracy.

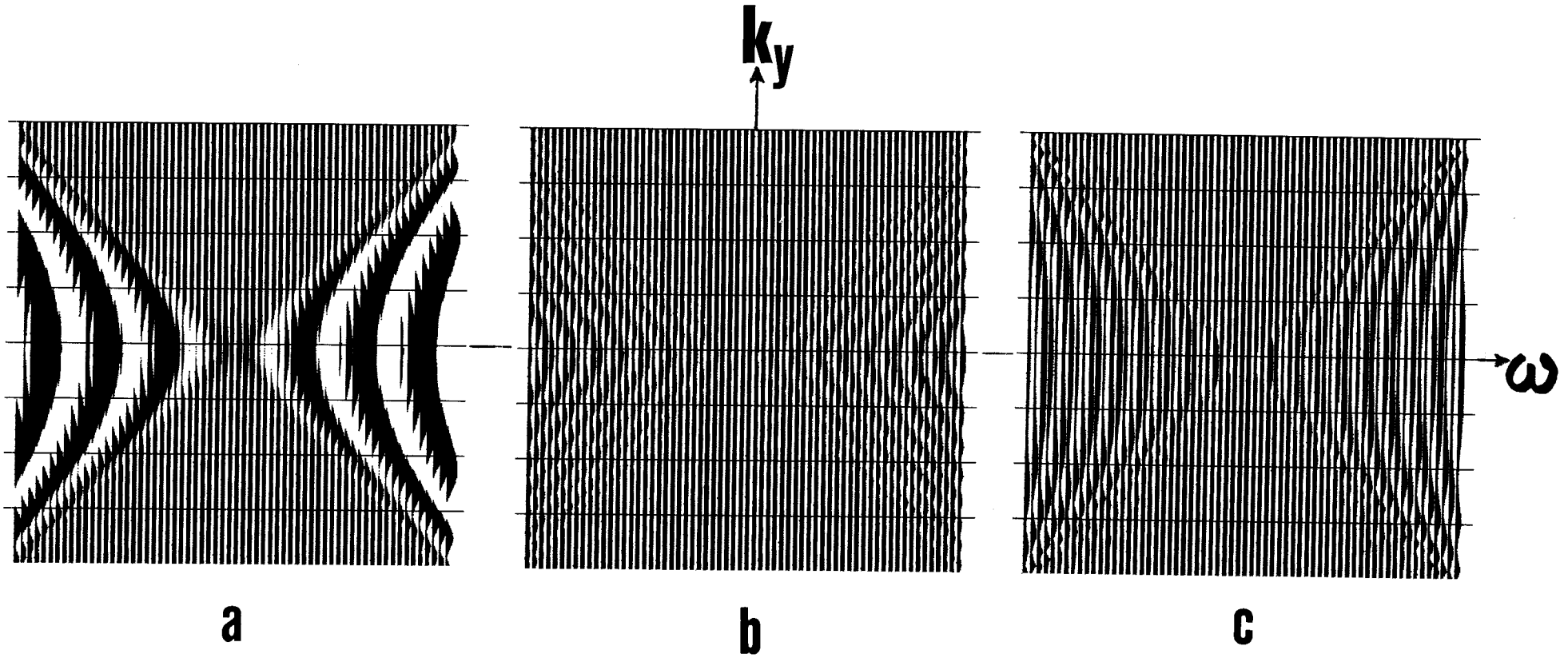

FIG. 1-2. Real part of (ω, k_y) -plane at z = 200 m. (a) DSR with h = 0 m, (b) DSR with h = 400 m, and (c) Sep with h = 400 m. Region of propagation widens as temporal frequency increases.

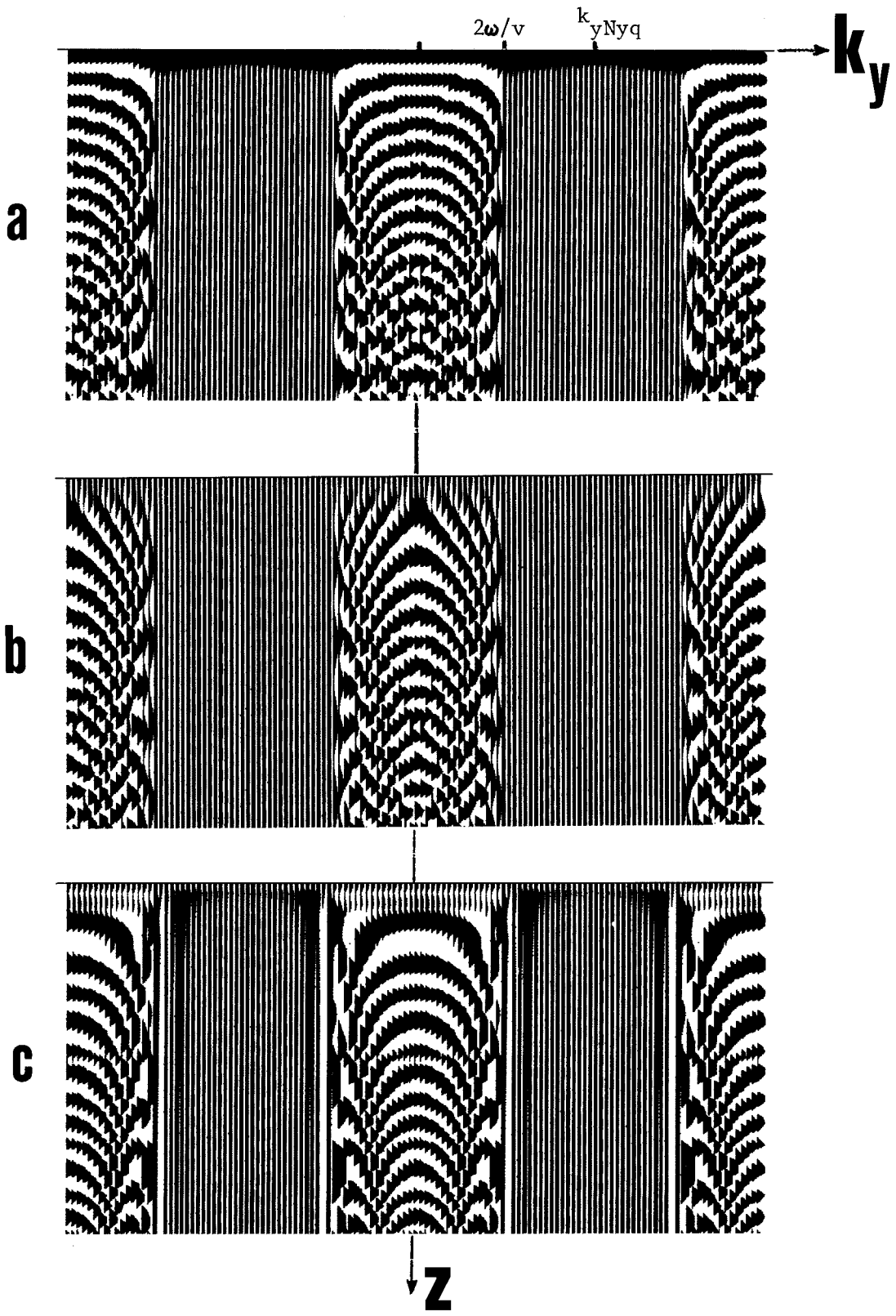

FIG. 1-3. Real part of (k_y,z) -plane at ω = 16 Hz. (a) DSR with h = 0 m, (b) DSR with h = 400 m, and (c) Sep with h = 400 m. Transition to evanescent energy occurs at $k_y = 2\omega/v$.

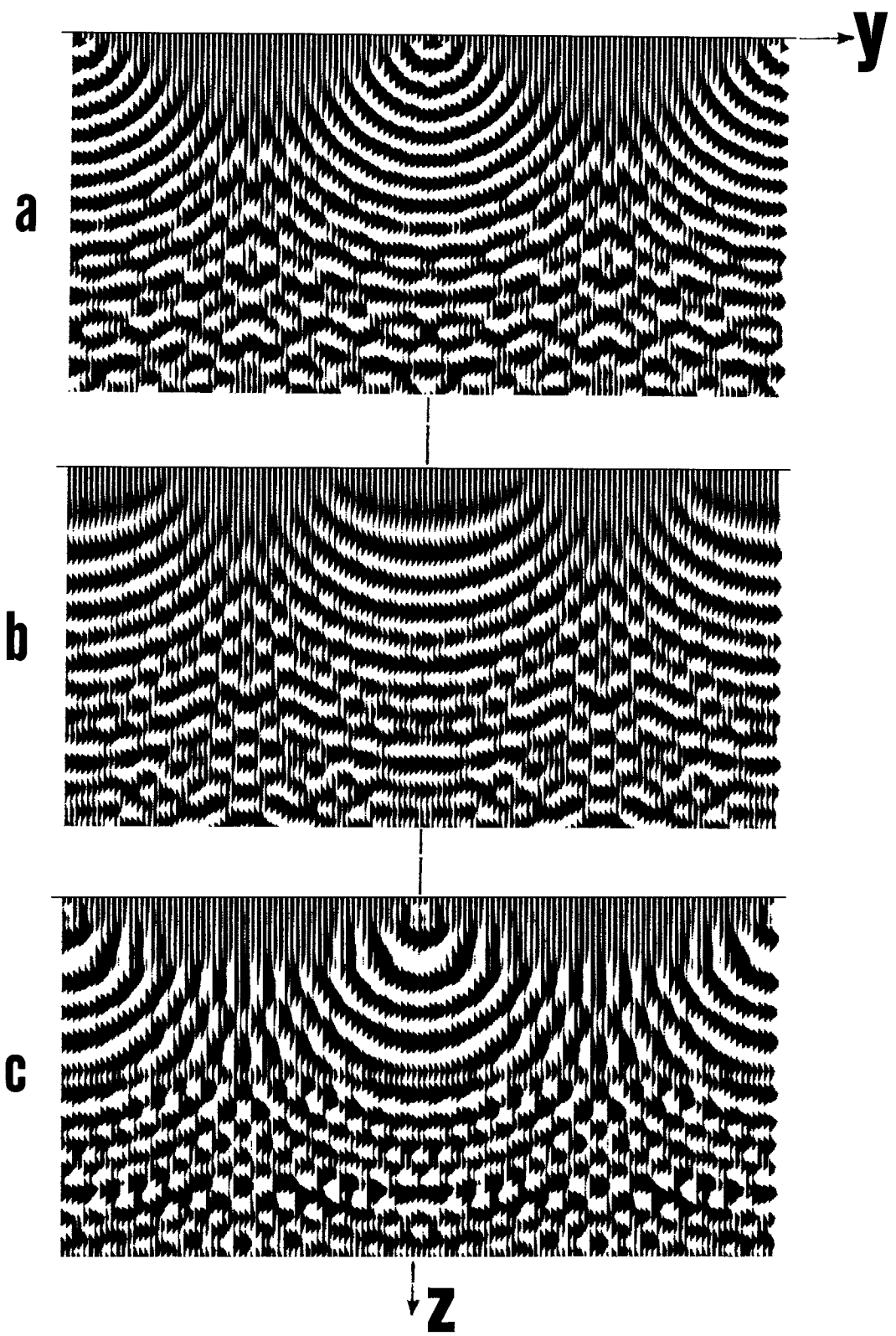

FIG. 1-4. Real part of (y,z) -plane at ω = 16 Hz. (a) DSR with h = 0 m, (b) DSR with h = 400 m, and (c) Sep with h = 400 m. Note the semi-circular wavefronts for h = 0 in (a) turn into semi-elliptical wave-fronts for h = 400 m in (b). The Sep operator fails to simulate the semi-elliptical wavefronts. Physically, the top frame is a picture of waves passing through point apertures spaced evenly along the y-axis.

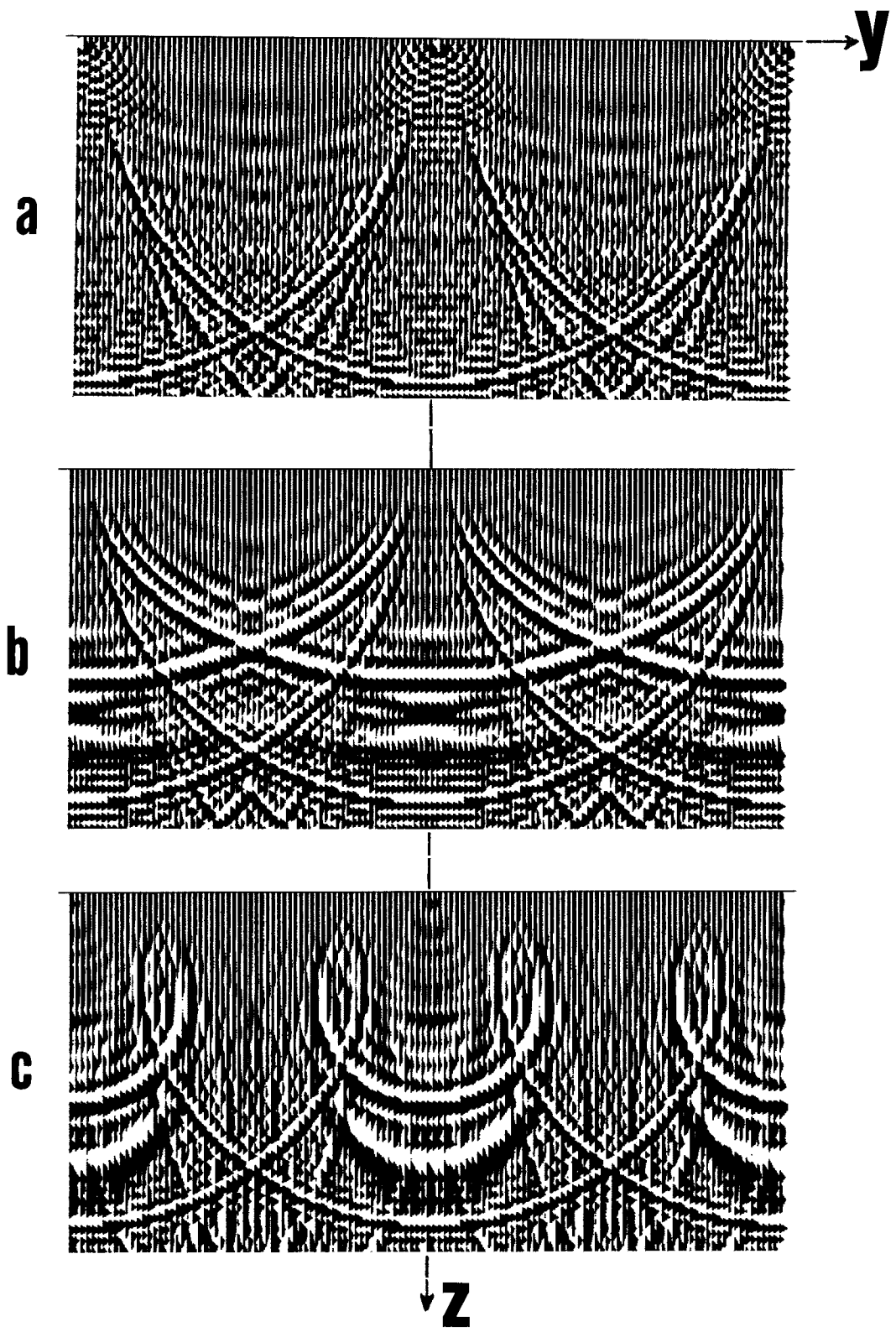

FIG. 1-5. Real part of (y,z) -plane at t = 1.024 sec. (a) DSR with h = 0 m, (b) DSR with h = 400 m, and (c) Sep with h = 400 m. Due to wraparound in h, we observe two wavefronts in (b) and (c), one for h = 400 m and one for h = 1200 m.

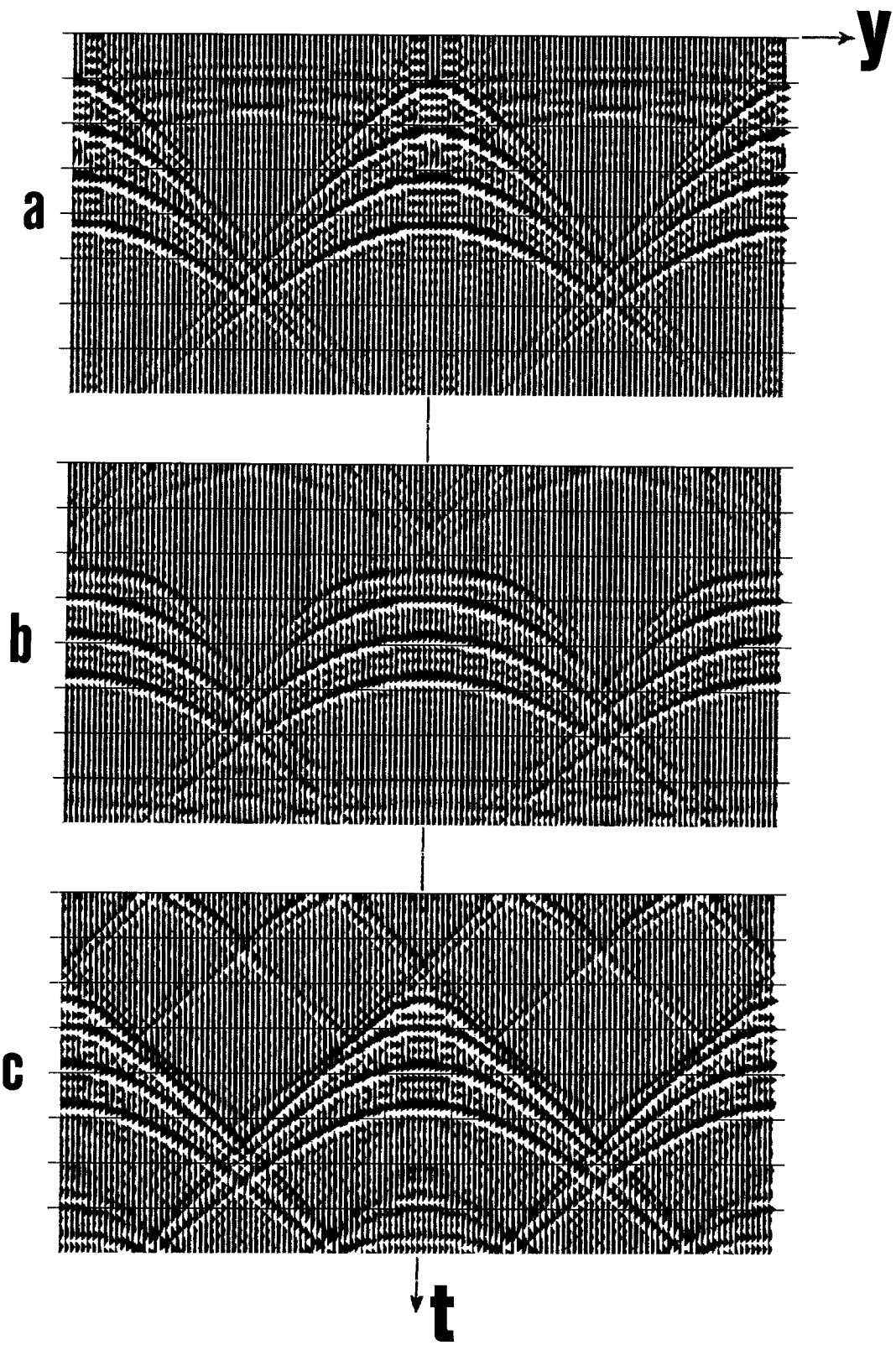

FIG. 1-6. Real part of (y,t) -planes at z = 200, 400, 600, and 800 m superimposed. (a) DSR with h = 0 m, (b) DSR with h = 400 m, and (c) Sep with h = 400 m. These frames represent impulse responses of DSR and Sep operators to point scatterers buried at the depths indicated. Loci of arrival times can be determined via stationary phase approximation to DSR and Sep operators as described in Appendix B (Sections B-1 and B-3).